PHYSICAL REVIEW B VOLUME 24, NUMBER 15 15 DECEMBER 1981

# Simplified theory of dislocation damping including point-defect drag. II. Superposition of continuous and pinning-point-drag effects

A. V. Granato

*Department of Physics and Materials Research Laboratory, University of Illinois at Urbana-Champaign, Urbana, Illinois 61801 and Institut für Allgemeine Metallkunde und Metallphysik, Technische Hochschule, Aachen, Germany*

Kurt Lücke

*Institute für Allgemeine Metallkunde und Metallphysik, Technische Hochschule, Aachen, Germany*

(Received 22 June 1981)

The combined effects which occur when two kinds of drag, one acting continuously along the dislocations and other at discrete points (point-defect drag), are derived. It is found that the damping and modulus change can always be expressed in good approximation as the sum of two Debye relaxations. For widely separated relaxation times, one corresponds to the point-defect drag and the other to continuous drag acting on the in-between loops. Expressions are given for the relaxation times and strengths for each of the two components for any number of movable pinning points. It is shown that the characteristic pinning-point-drag effects have nothing to do with whether the drag acts continuously or at discrete points, but depend on the fact that the movable pinners exert restoring and viscous forces which act only on a part of the dislocation displacement.

## I. INTRODUCTION

This article deals with dislocation damping arising from sources which provide both continuous drag and pinning-point drag simultaneously. It makes use of results given in the preceding article[1] (here referred to as paper I), which are first summarized.

(i) Using only physical arguments without calculations, a simplified theory of dislocation damping due to point-defect drag was presented. It consists of an application of the Granato-Lücke formulas originally derived as approximations for the case of continuous drag,[2,3] and also for the case of point-defect drag, and leads to a description of the internal-friction effects as a simple Debye relaxation with relaxation strength $\Delta$ and relaxation time $\tau$ given by

$$\Delta=\frac{\Lambda G b^2}{\kappa}\frac{L^2}{12C},\quad \tau=\frac{B}{\gamma}\frac{L^2}{12C}\ . \qquad (1)$$

Here $G$ is the shear modulus, $b$ the Burgers vector, $\Lambda$ the dislocation density, $C$ the dislocation line tension, $L$ the loop length, and $B$ a properly defined drag constant. The parameters $\kappa$ and $\gamma$ are numerical factors of the order of unity. They correspond to (but are somewhat differently defined from) those introduced by Lenz and Lücke[4] in order to obtain a more general form of writing these equations.

(ii) An exact calculation of $\Delta$ and $\tau$ for drag due to equidistant pinning points was carried out as a function of the number $p=n-1$ of pinning points per loop including the case of continuous pinning with $p=\infty$. The results deviate somewhat from an exact Debye relaxation and from Eq. (1), which represents nevertheless a good approximation to the exact result. The factors $\kappa$ and $\gamma$ change by small amounts with $p$, but still by only 33% for the most extreme case of $p=1$.

(iii) Different Debye-type approximations to the exact solutions were defined both for continuous and point defect drag (low-frequency, frequency, Fourier, and zero-order approximations). For all of them the relaxation strength and time are again given by Eq. (1). They differ only in numerical factors $\kappa$ and $\gamma$, but by less than 20%. This is in general range of accuracy of the simplified theory.

(iv) Besides generalizing and simplifying the string theory to include drag effects, the theory was further generalized and simplified to include string effects within the framework of a rigid-rod theory.

 

In this article the expected superposition phenomena are again first derived without calculation (Sec. II) by using only physical arguments and applications of the old Granato-Lücke formulas. Section III gives a mathematical treatment but for the simple rigid-rod model,[5] for which both the restoring forces and the drag forces—also those due to point defects—are considered to act continuously. Because of its mathematical transparency, this model is especially well suited to demonstrate the underlying physics of the effects. In Sec. IV, finally, the string model is treated, in which it is assumed that both the restoring forces and the drag due to the point defects act at discrete points.

It is found that all three treatments give rather similar results. The damping and modulus changes can always be expressed in good approximation as the sum of two Debye-type relaxations. With these results, a fuller understanding of the basic physics of the drag effect is also obtained. It is found that the characteristic effects for pinning-point drag have nothing to do with whether the movable point defects act continuously or at discrete points. They depend instead on the fact that the movable pinners exert both restoring and viscous forces which act only on a part of the dislocation displacement.

## II. SIMPLIFIED DESCRIPTION OF THE SUPERPOSITION OF THE TWO DRAGS BY THE GRANATO-LÜCKE FORMULAS

The dislocation equation of motion

$$B\frac{\partial y}{\partial t}+C\frac{\partial^2 y}{\partial x^2}=b\sigma \tag{2}$$

leads, for periodic external stresses $\sigma=\sigma_0\exp(i\omega t)$, to a relaxation behavior that can be well approximated as that of Debye type with relaxation strength $\Delta$ and relaxation time $\tau$ given by the Granato-Lücke formula equation (1). In Eq. (2), $x$ is the coordinate along the dislocation, $y(x,t)$ is its displacement, and the inertial term has been neglected. This was known before for the case of continuous drag where one obtains from Eq. (1) with $L=L_N$ and $B=B_c$

$$\Delta_N=\frac{\Lambda G b^2}{\kappa_N}\frac{L_N^2}{12C},\quad \tau_N=\frac{Bc}{\gamma_N}\frac{L_N^2}{12C}\ . \tag{3}$$

For the case of pinning-point ("discrete") drag, it has been shown in paper I that one must take $L=L_N$ and $B=B_d$ in Eq. (1) to obtain

$$\Delta_d=\frac{\Lambda G b^2}{\kappa_d}\frac{L_N^2}{12C},\quad \tau_d=\frac{B_d}{\gamma_d}\frac{L_N^2}{12C}\ . \tag{4}$$

As will be shown in present paper, for the case of superposition of both continuous and discrete drag, an additional relaxation process will occur given again by Eq. (1) but with $L=L_d$ and $B=B_c$ as

$$\Delta_c=\frac{\Lambda G b^2}{\kappa_c}\frac{L_d^2}{12C},\quad \tau_c=\frac{Bc}{\gamma_c}\cdot\frac{L_d^2}{12C}\ . \tag{5}$$

In the above equation $L_N$ is the distance between fixed network pinning points, $L_d=L_N/n$ where $n-1=p$ is the number of movable pinning points per network length $L_N$, and $B_d$ is the drag constant for pinning-point drag, given by

$$B_d=\frac{1}{mL_d}=\frac{n}{mL_N},\quad m=\frac{D}{kT} \tag{6}$$

where $m$ is the mobility and $D$ the diffusion coefficient for diffusion of the movable pinning points with the dislocation.

In the treatment of the effect of movable pinning points given in paper I it is assumed that no continuous drag exists, so that only the drag force due to the pinning points dragged along by the moving dislocation (Fig. 1) has to be considered. This treatment, which seems to suggest that the only influence of movable pinning points is to exert drag [first term in Eq. (2)] on the dislocation misses, however, two important features. They are connected with the facts that, even for infinite $B_d$, the dislocation motion is not completely suppressed and that the pinners also cause a restoring force [second term in Eq. (2)] for the dislocation. This is shown in Fig. 1, which indicates that there are two components to the response of the dislocation, one ($y_d$) corresponding to the motion of the movable pinners and the other ($y_c$) to the motion of the segments $L_d$ between the pinners. First, two limit cases (i) and (ii) will be considered.

(i) Here it is assumed that $B_d \ll B_c$, i.e., the pinners are able to follow the dislocation motion rather fast, so that the displacement is given nearly by that of a dislocation without pinners [$y=y_N$, Fig. 1(a)]. This means that, in this case, the role of the pinners is principally to produce some drag with very little change of the restoring force. The latter remains about the same as for the free dislocation corresponding to the loop length $L_N$. Thus one has essentially the original Granato-Lücke form for a damping peak, which is given by Eq. (3), but with a drag constant slightly larger than $B_c$.

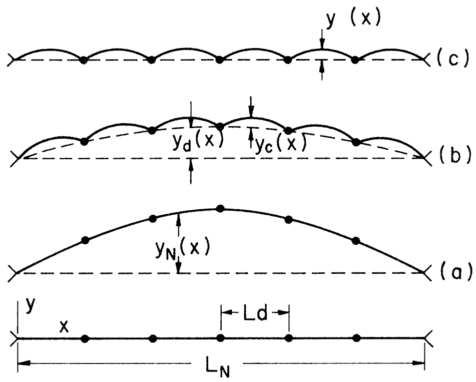


FIG. 1. Schematic representation of dislocation displacement $y$ as a function of the coordinate $x$. $L_d$ is the distance between pinning points. $L_N$ is the distance between immovable pinning points. (a) Displacement $y_N(x)$ for $B_d << B_c$, where $B_d$ is the discrete pinning-point drag and $B_c$ is the continuous drag. The pinners are able to follow the dislocation line. (b) Displacement $y(x)=y_d(x)+y_c(x)$ for $B_d >> B_c$ and low frequencies. $y_d(x)$ is the displacement of the pinning points and $y_0$ is the displacement of the dislocation segments between the pinning points. The pinners are able to move at low frequencies. (c) Displacement for $B_d >> B_c$ and high frequencies. The pinners move only slightly.

(ii) Now it is assumed that $B_d >> B_c$. Then at high frequencies, the pinners move only slightly and dislocation motion is mainly caused by the in between loops [Fig. 1(c)]. Here the pinners contribute only slightly to the drag but increase the restoring force to a value nearly that corresponding to $L_d$. Since the drag on these segments is of the usual continuous nature, i.e., $B = B_c$, a damping peak arises again, described by Eq. (5). At frequencies low enough to cause a motion of, and thus also a damping by, the pinning points, [Fig. 1(b)], the pinners influence both the drag and the restoring force. Because $B_c << B_d$, the in-between loops are practically in phase here with the applied stress, so that their motion contributes fully to the modulus but only slightly to the damping. This means that at these frequencies one obtains the modulus defect due to the motion of the in between segments $L_d$, superimposed on a relaxation process described in Eq. (4) which is caused by the pinning-point motion.

Thus, associated with the two contributions to dislocation motion, the internal-friction effects for $B_d >> B_c$ consist of two relaxation processes, one due to the motion of pinning points [Eq. (4)] and one due to the motion of the in between segments $L_d$ [Eq. (5)]:

$$\delta=\delta_d+\delta_c, \quad \phi=\phi_d+\phi_c . \tag{7}$$

In Eq. (7) $\delta \equiv Q^{-1}$ is the damping and $\phi \equiv \Delta M/M$ is the relative modulus change, where $M$ is the modulus.

The frequency dependence of these internal-friction effects is plotted in Fig. 2. For case (i) ($B_d << B_c$), one has only a single relaxation peak, given by Eq. (3) and shown by the solid line. For case (ii) ($B_d >> B_c$), two well-separated maxima occur, given in Eqs. (4) and (5) and shown by the dashed lines. According to Eqs. (4) and (5) the height of the peaks does not depend upon $B_d$ or $B_c$, and the second peak is smaller than the first by a factor $L_N^2/L_d^2=n^2$. For the case of two well-separated peaks, the total relaxation strength is the same as that for the single peak, as can be seen in the figure for the low-frequency modulus limit. Also, for cases (i) and (ii), the asymptotic value of the decrement at high frequency is the same. If one decreases $B_c$ towards zero (vanishing continuous drag), $\tau_c$ goes to zero, i.e., the damping peak $\delta_c$ would move to infinite frequency without changing its height. This means that no contribution to the damping but a full reduction of the modulus occurs at finite frequency for the second peak. If one increases $B_d$ indefinitely (firm pinning points), $\tau_d$ becomes infinite, i.e., the damping peak $\delta_d$ moves to infinitely small frequency. With decreasing $B_d$, i.e., increasing mobility of the pinning points, this peak moves to higher frequency without changing its height. When $B_d$ becomes much smaller than $B_c$, the two peaks $\delta_d$ and $\delta_c$ must combine in some way to become the single peak $\delta_N$, but the surprising way that this occurs cannot be seen in this simple way (see Sec. IV).

These results concerning the superposition of continuous and point-defect drag have again been obtained directly from the Granato-Lücke formulus without any calculations. They describe correctly the basic physics of these processes. Quantitatively, these results are only approximations, as are the Granato-Lücke formulas themselves. In the two following sections a more thorough investigation of this superposition effect is undertaken.

## III. SUPERPOSITION OF DRAG EFFECTS IN THE RIGID-ROD MODEL

According to the preceding section, the two drag effects described there cannot be superimposed

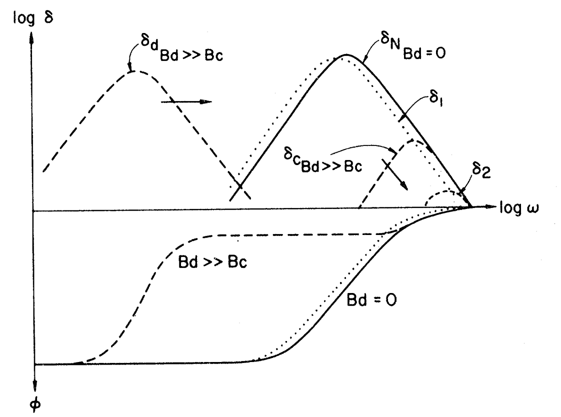


FIG. 2. Frequency dependence of the decrement $\delta$ and modulus change $\phi$. For $B_d << B_c$, there is only a single relaxation $\delta_N$. For $B_d >> B_c$, there are two peaks $\delta_d$ and $\delta_c$. The total relaxation strength is the same as that for the single peak so that the total modulus change at low frequencies is the same for both cases. Also the asymptotic value of the decrement at high frequencies is the same.

simply by superposition of the drag constants ($B = B_c + B_d$). The reason for this fact does not lie in the discrete nature of the drag due to movable pinning points, but in their influence upon the restoring force. This will be demonstrated with exact calculations for a simplified model proposed by Lücke, Schnell, and Sokolowski,[5] for which the pinning-point drag is also treated continuously. It is based on the rigid-rod model of dislocation motion, which, as has been shown recently by Lenz and Lücke[4] and by Granato[6] and also in paper I (Sec. V), gives a good approximation to the dislocation behavior resulting from the vibrating-string model.

In the rigid-rod model [Fig. 3(a)], it is assumed that the dislocation possesses a constant displacement $y(t)$ over its whole length and that it experiences per unit length a restoring force $-K_N y$ and a frictional force $-B_c \dot{y}$. It is here further assumed that there are point defects which all have the same displacement $y_d(t)$ and which exert an additional force per unit length $-K_d(y-y_d)$. This means that the point defects can be thought of as being continuously distribution along the displacement line $y_d$. In Fig. 3(b) the forces acting on the dislocation are represented by simple springs and dashpots. Again neglecting the inertia terms, one obtains for the motion of the dislocation

$$B_d \dot{y} + K_N y + K_d(y - y_d) = b\sigma_0 \exp(i\omega t) \tag{8}$$

and for the motion of the line of the point defects

$$B_d \dot{y}_d - K_d(y - y_d) = 0 \ . \tag{9}$$

Here the subscript $N$ refers to the restoring force due to the loop length $L_N$ and subscript $d$ to restoring and drag forces due to point defects with the loop length $L_d$. The equations, however, are set up as if all the forces were of continuous and not of discrete nature. The solution of this set of differential equations is given and discussed in Appendix A. It leads to a superposition of two Debye-type processes denoted here by the indices 1 and 2:

$$\delta = \delta_1 + \delta_2 = \frac{\Delta_1 \omega \tau_1}{1+\omega^2\tau_1^2} + \frac{\Delta_2 \omega \tau_2}{1+\omega^2\tau_2^2} \ , \tag{10a}$$

$$\phi = \phi_1 + \phi_2 = \frac{\Delta_1}{1+\omega^2\tau_1^2} + \frac{\Delta_2}{1+\omega^2\tau_2^2} \ . \tag{10b}$$

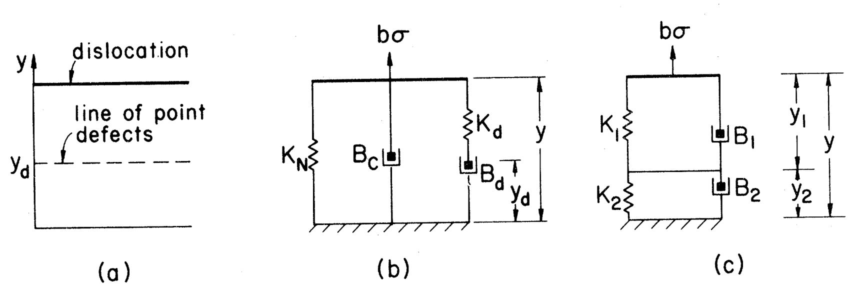


FIG. 3. Schematic representation of the displacement $y$ of a dislocation in a rigid-rod model under an applied stress. The dislocation is subject to a continuously applied (1) restoring force ($-K_N y$), (2) viscous force ($-B_c y$), and (3) drag force by point defects [$-K_d(y-y_d)$], where $y_d$ is the point-defect displacement. In (b), the forces acting on the dislocation are represented by simple springs and dashpots. Figure (b) is equivalent to (c), where $K_{1,2}$ and $B_{1,2}$ are given by Eqs. (18). From (c) one sees that there are two independent relaxations of the system.

In analogy to the effects occuring during coupled vibrations, these two processes will be referred to as the "normal modes" of the relaxation system. The relaxation times and relaxation strengths are given by

$$\tau_{1,2}=\frac{\tau_0}{2}\left([1+\mu(1+1/\lambda)] \pm\{[1+\mu(1+1/\lambda)]^2-4\mu/\lambda\}^{1/2}\right), \quad (11a)$$

$$\Delta_{1,2}=\frac{\Delta_0}{2}\left[1\pm\frac{1+\mu(1-1/\lambda)}{\{[1+\mu(1+1/\lambda)]^2-4\mu/\lambda\}^{1/2}}\right], \quad (11b)$$

with

$$\lambda=K_d/K_n,\quad \mu=B_d/B_c\ . \quad (12)$$

The quantities

$$\Delta_0=\frac{\Lambda Gb^2}{K_N},\quad \tau_0=\frac{B_c}{K_N} \quad (13)$$

are those which would be obtained without any point defects ($\mu=0$). For $\mu=B_d/B_c<<1$, one obtains

$$\Delta_1=\Delta_0=\frac{\Lambda Gb^2}{K_N},\quad \tau_1=\tau_0=\frac{B_c}{K_N}\ , \quad (14a)$$

$$\Delta_2=\frac{\Lambda Gb^2}{K_d}\left[\frac{B_d}{B_c}\right]^2,\quad \tau_2=\frac{B_d}{K_d}\ , \quad (14b)$$

while for $\mu>>1$

$$\Delta_1=\frac{\Lambda Gb^2}{K_N(1+K_N/K_d)},\quad \tau_1=\frac{B_d}{K_N}(1+K_N/K_d)\ , \quad (15a)$$

$$\Delta_2=\frac{\Lambda G_b^2}{K_d(1+K_N/K_d)},\quad \tau_2=\frac{B_c}{K_d(1+K_N/K_d)}\ . \quad (15b)$$

As shown in paper I, the restoring force for a string fixed at its end is given by

$$K_N=\frac{12C}{L_N^2}\ \text{and}\ K_d=\frac{12C}{L_d^2} \quad (16)$$

for the loop lengths $L_N$ and $L_d$, respectively. Introducing this into Eqs. (14a), (15a), and (15b), these results closely resemble those of Eqs. (3), (4), and (5). Thus

$$\delta_1=\delta_N\ \text{and}\ \delta_2\rightarrow 0\ \text{for}\ \mu<<1\ , \quad (17a)$$
$$\delta_1=\delta_d\ \text{and}\ \delta_2=\delta_c\ \text{for}\ \mu>>1\ .$$

They become identical if the following values for the numerical factors are used:

$$\kappa_N=\gamma_N=1,\quad \kappa_d=\kappa_c=1+1/\lambda\ ,$$
$$\gamma_d=\frac{1}{1+1/\lambda},\quad \gamma_c=1+1/\lambda\ . \quad (17b)$$

For the usually considered range of $\lambda\geq 4$ (i.e., $L_d/L_N\leq 2$), these factors remain near unity, as anticipated. Values for other limiting cases are also given in Table II, cited in Appendix A.

Figure 4 shows $\tau_{1,2}/\tau_0$ and $\Delta_{1,2}/\Delta_0$ as a function of $\mu$ for the special case $\lambda=3$. One recognizes that peak 1 is the main relaxation peak. Peak 2, which is located at higher frequencies, is completely negligible for $\mu<<1$. For $\lambda>>1$ it is small compared to peak 1 also in the range $\mu>>1$. It is interesting to note that the peaks are not to be associated one with continuous drag and the other with point-defect drag. Instead, peak 1 describes both effects, whereas peak 2 represents only a usually small correction. For $\mu<<1$, peak 1 describes the

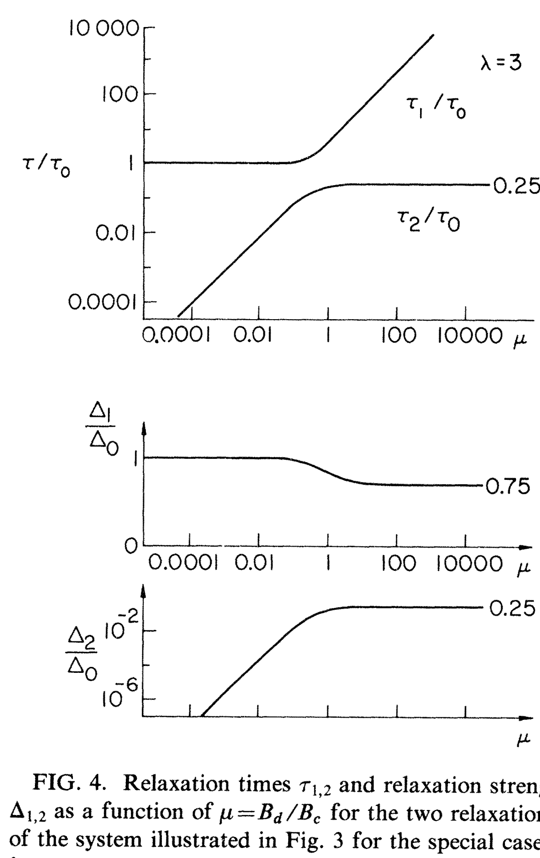


FIG. 4. Relaxation times $\tau_{1,2}$ and relaxation strength $\Delta_{1,2}$ as a function of $\mu=B_d/B_c$ for the two relaxations of the system illustrated in Fig. 3 for the special case of $\lambda=K_d/K_n=3$. $\tau_0$ is given by $B_c/K_N$ and $\Delta_0$ by $\Lambda Gb^2/K_N$. Peak 1 is the main peak and the total relaxation strength is always $\Delta_0$.

effect of continuous drag, and for $\mu >> 1$ that of point-defect drag. For $\mu \approx 1$ the effects are mixed, and the relaxation times $\tau_1$ and $\tau_2$ do not cross. The way in which the peaks combine for $B_d \rightarrow 0$ is illustrated in Fig. 2 by the dotted curves. One sees that $\delta_c$ disappears by shifting downward along the high-frequency asymptote of $\delta_N$. The peak $\delta_d$ picks up the extra relaxation strength lost by $\delta_c$. From Eqs. (11)–(15) some results anticipated earlier on physical ground (Sec. II) can easily be derived. The total relaxation strength is always the same, $\Delta_1 + \Delta_2 = \Delta_0$, i.e., equal to the modulus defect obtained without any frictional forces. In addition, the high-frequency asymptote for $\delta$ is exactly given by $\Delta_0/\omega\tau_0$, completely independent of $\lambda$ and $\mu$. This expresses the fact that at sufficiently low frequencies the dislocation displacement is limited by $K_N$, and at sufficiently high frequencies the dislocation motion is limited by the drag force $B_c$.

Finally, it may be seen from this example that the existence of two relaxations with two different relaxation times does not depend on whether the point-defect drag acts continuously or discretely. It depends only on the fact that the movable pinning points provide forces, restoring and viscous, which act only on part of the total displacment. The simple spring circuit in Fig. 3(b) is equivalent to that of Fig. 3(c), which is a series connection of two simple parallel circuits of springs and dashpots. The equivalent restoring and viscous constants $K_1$, $K_2$, $B_1$, and $B_2$ are then defined by the expressions

$$\Delta_{1,2} = \frac{\Lambda G b^2}{K_{1,2}}, \quad \tau_{1,2} = \frac{B_{1,2}}{K_{1,2}}, \tag{18a}$$

so that one obtains with Eq. (13)

$$K_{1,2} = \frac{\Lambda G B^2}{\Delta_{1,2}}, \tag{18b}$$

$$B_{1,2} = K_{1,2}\tau_{1,2} = \Lambda G b^2 \frac{\tau_{1,2}}{\Delta_{1,2}}, \tag{18c}$$

where $\Delta_1$, $\Delta_2$, $\tau_1$, and $\tau_2$ are given by Eq. (11). This gives a precise answer to the question raised at the beginning of this section, i.e., to what extent do movable pinners act as a source of extra restoring force or as extra drag? In general, they do both and the amounts of each are given by Eq. (18).

## IV. SUPERPOSITION OF DISCRETE AND CONTINUOUS DRAG FOR THE VIBRATING STRING MODEL

We now supppose that a continuous drag $B_c$ acts on a dislocation segment length $L_N$ pinned firmly at its ends, and that $n-1$ movable pinners are at points separated by lengths $L_d = L_N/n$ (Fig. 1). The Debye-type response for this system can be calculated most simply for the zero-order approximation. This is done in Appendix C, where the relaxation times and relaxation strengths are found to be

$$\tau_{1,2} = \frac{\tau_0}{2}\{(1+\mu/\gamma) \pm [(1+\mu/\gamma)^2 - 4(\mu/\gamma)/n^2]^{1/2}\} \tag{19a}$$

$$\Delta_{1,2} = \frac{\Delta_0}{2}\left[1 \pm \frac{1+(1-2/n^2)(\mu/\gamma)}{[(1+\mu/\gamma)^2 - 4(\mu/\gamma)/n^2]^{1/2}}\right], \tag{19b}$$

where

$$\Delta_0 = \frac{\Lambda G b^2 L_N^2}{12C}, \quad \tau_0 = \frac{B_c L_N^2}{12C}, \tag{20a}$$

$$\mu = \frac{B_d}{B_c}, \quad \tau_d = \frac{B_d L_N^2}{\gamma 12C} = \tau_0(\mu/\gamma), \tag{20b}$$

and $\gamma = \gamma_0(n) = n/(n-1)$ is a numerical factor [c.f. Eq. (1)] defined for the zero-order approximation in paper I. The limit values following from Eqs. (19) for either $B_c << B_d$ or $B_c >> B_d$ are listed in Table I. Since Eqs. (19) are derived using the zero-order approximation, they are valid for $\gamma(n) = \gamma_0(n) = n/(n+1)$. By comparing Table I and Table I of paper I, one recognizes, however, that for both limit cases of $\mu$, the quantities $\tau_1$ and $\Delta_1$ have exactly the form valid for the low-frequency approximation if one replaces $\gamma_0(n)$ by $\gamma_L(n)$. Thus it can be suspected that Eqs. (19) also give a rather good description of the low-frequency approximation for finite $\mu$. Since the first-term Fourier approximation is very close to the low-frequency approximation, Eqs. (19) should also be rather well applicable for this approximation if one sets $\gamma = \gamma_F(n)$. For the high-frequency approximation, however, Eqs. (19) are less useful since there the value resulting for $\Delta_1$ for $B_c = 0$ no longer agrees with that given in Table I, even for $\gamma = \gamma_H$.

It is easily noted that the structure of Eqs. (19) are similar to those of Eqs. (11) for the rigid rod.

They become identical if one makes the following replacements in Eqs. (11):

$$K_N \to \frac{12C}{L_N^2}, \quad \lambda \to n^2-1, \quad \mu_R \to \mu \frac{1-1/n^2}{\gamma_0(n)} . \tag{21}$$

Because of this correspondence, the discussion given in Sec. III for the rigid-rod model is likewise valid for the string model. Thus Fig. 4 for $\alpha=3$ represents the double-loop $n=2$ case. Equation (17a), giving a correlation between the rigid-rod relaxation and those relaxations described by Eqs. (3)–(5), is also valid for the string model. However, instead of the numerical factors in Eq. (17b), the following factors derived by comparison of Table I and Eqs. (20) with Eqs. (3)–(5) apply:

$$\kappa_N=\kappa_c=1, \quad \gamma_n=\gamma_c=1 , \tag{22a}$$

$$\kappa_d=\frac{1}{1-1/n^2}, \quad \gamma_d=\frac{1}{1+1/n} . \tag{22b}$$

These factors agree with those listed in Table I of paper I for the zero-order approximation [Eq. (22a for the continuous case $n=\infty$ and Eq. (22b) for the discrete case]. They do not agree, however, with those given by Eq. (17b) if $\lambda$ is expressed simply by Eq. (16) and $B_d$ by Eq. (6). This is due to differences in the geometry of the rigid-rod and the string vibration, similar to that found in Sec. V of paper I.

A very useful approximation covering the whole range of $n$ and $\mu$ can be derived by expanding Eqs. (19) and introducing $\mu/\gamma=\tau_d/\tau_0$ [Eq. (21)] to give

$$\tau_1=(\tau_0+\tau_d)\left\{1-\frac{\tau_0\tau_d}{n^2(\tau_0+\tau_d)^2}+\cdots\right\}, \tag{23a}$$

$$\frac{1}{n^2\tau_2}=\left[\frac{1}{\tau_0}+\frac{1}{\tau_d}\right]\left\{1+\frac{\tau_0\tau_d}{n^2(\tau_0+\tau_d)^2}+\cdots\right\}. \tag{23b}$$

The largest value the second term in the curly brackets can have is when $n=2$ and $\tau_d/\tau_0=1$ and is $\frac{1}{16}$. Similarly Eqs. (19b) gives

$$\Delta_1=\Delta_0\left\{1-\frac{\tau_d^2}{n^2(\tau_0+\tau_d)^2}+\cdots\right\}, \tag{24a}$$

$$\Delta_2=\Delta_0\frac{\tau_d^2/\tau_0^2}{n^2(1+\tau_d/\tau_0)^2}+\cdots . \tag{24b}$$

Here the second term is always $<\frac{1}{4}$. This means the curly brackets can be taken as unity with a maximum error of 7% or 25%, respectively.

The partial relaxations $\delta_1$ and $\delta_2$ (normal modes) can also be calculated for the string case according to Fig. 3(c). The corresponding restoring force and drag constants are again obtained from Eqs. (18), where now Eqs. (19) must be used for $\tau_{1,2}$ and $\Delta_{1,2}$. In particular, for the main relaxation peak $\delta_1$ one recognizes that $K_1=\Lambda G b^2/\Delta_1$ changes relatively little with varying $\mu$: For the limit case $n=\infty$, $K_1$ is independent of $\mu$, and for other limit case $n=2$, $K_1$ increases by factor of $\frac{4}{3}$ when $\mu$ goes from 0 to $\infty$. For the drag constant $B_1$, however, large changes are obtained. Good approximate descriptions for these quantities, valid over the whole range of $\mu$ and $n$, are found by introducing Eqs. (23a) and (24a) into Eqs. (18). In particular, for $B_1$ one obtains

$$B_1=\Lambda G b^2\frac{\tau_1}{\Delta_1}=\frac{\tau_0+\tau_d}{\tau_0}\left[1-\frac{\tau_d(\tau_0-\tau_d)}{n^2(\tau_0+\tau_d)^2}\right]$$

$$=\left[B_c+\frac{B_d}{\gamma}\right]\left[1-\frac{\frac{B_d}{\gamma}\left[B_c+\frac{B_d}{\gamma}\right]}{n^2\left[B_c+\frac{B_d}{\gamma}\right]^2}\right] . \tag{25}$$

TABLE I. Limit values for relaxation times and strength for a string with $n-1$ movable pinners. $\tau_0=B_cL_N^2/12C$, $\Delta_0=\Lambda G b^2 L_N^2/12C$, $\mu=B_d/B_c$, $\gamma_0=1/(1+1/n)$.

| | $\tau_1/\tau_0$ | $\tau_2/\tau_0$ | $\Delta_1/\Delta_0$ | $\Delta_2/\Delta_0$ |
|---|---|---|---|---|
| $\mu<<1$ | $1+\left[1-\frac{1}{n^2}\right]\frac{\mu}{\gamma}$ | $\frac{1}{n^2}\frac{\mu}{\gamma}$ | $1-\frac{\Delta_2}{\Delta_0}$ | $\frac{n^2-1}{n^4}\left[\frac{\mu}{\gamma}\right]^2$ |
| $\mu>>1$ | $\frac{\mu}{\gamma}+\left[1-\frac{1}{n^2}\right]$ | $\frac{1}{n^2}$ | $1-\frac{\Delta_2}{\Delta_0}$ | $\frac{1}{n^2}-\frac{2(n^2-1)}{n^4}\frac{\gamma}{\mu}$ |

For $n=\infty$ (i.e., $\gamma=1$), this gives

$$B_1=B_c+B_d\ , \tag{26a}$$

and for the other limit case $n=2$,

$$B_1=(B_c+\tfrac{3}{2}B_d)\left[1-\frac{3}{8}\frac{B_d(B_c-\frac{3}{2}B_d)}{(B_c+\frac{3}{2}B_d)^2}\right]. \tag{26b}$$

For general $n$ Eq. (25) leads to the three limit cases

$$B_1\begin{cases} B_c+(1-1/n^2)\dfrac{B_d}{\gamma}, & B_c>>B_d \\ 2B_c, & B_c=B_d/\gamma \\ \dfrac{1-3/n^2}{1-1/n^2}B_c+\dfrac{1}{1-1/n^2}\dfrac{B_d}{\gamma}, & B_c<<B_d/\gamma\ . \end{cases} \tag{27}$$

It can easily be recognized that for these three cases the approximate equation (25), in fact, gives the exact values. This means that Eq. (25) represents an extremely good interpolation formula for the main drag constant $B_1$ over the whole ranges of $n$'s and $B$'s. From the calculations in Appendix C, one can also obtain the displacements $y_1(x)$ and $y_2(x)$, corresponding to the two relaxations. One finds that each of $y_1$ and $y_2$ contains, in general, a mixture of the dislocation displacement, corresponding to pinning-point motion and motion of the segments between pinning points. Only for $\mu=B_d/B_c>>1$ does $y_1$ represent the pinning-point displacement. The sum of $y_1$ and $y_2$ always gives the same full parabolic displacement function at low frequencies.

## V. SUMMARY

By superposition of continuous drag and drag due to movable point defects, a dislocation response characterized by the sum of two Debye-type relaxation processes is obtained. They can be considered as the "normal modes" of the relaxational system. The values for the corresponding relaxation strengths and relaxation times are derived by physical arguments in an approximate manner (Sec. II), by exact treatment of a model in which restoring and drag forces are assumed to act continuously along the dislocation (Sec. III), and by approximate treatment of a model in which these forces really act pointwise (i.e., the vibrating-string model with pinning-point drag, Sec. IV). All three treatments lead to very similar results.

The reason that superposition of continuous and point-defect drag does not result in a simple addition of the drag constants but in two separate Debye peaks is that the movable pinning points influence not only the drag force but also the restoring force. As can be derived, especially from the results for the continuous model, this behavior is not caused by the pointwise action of drag and/or restoring forces due to the point defects, but by the fact that they act on only part of the dislocation displacement.

The two resulting Debye-type relaxation processes are not attributed as one to continuous drag and the other to point-defect drag. Instead both are mixed. One of them, however (here characterized by the subscript 1), is always the main process while the other (subscript 2), which always lies at higher frequencies than the first, plays the role of a correction. The main peak $\delta_1$ always represents the motion of the whole loop length. The second peak $\delta_2$ can be recognized individually only for the case $B_d>B_c$, and then represents the relaxation due to the vibrations of the dislocation segments $L_d$ between the movable pinning points. For $B_d<<B_c$, the second peak disappears.

Very good analytical approximations [Eqs. (23) and (24)] can be derived for the relaxation strengths and times of these peaks. This confirms the results of Sec. II obtained by physical arguments that only the old Granato-Lücke formulas have to be applied to describe these peaks. In particular, one obtains for the main peak $\Delta_1\approx\Delta_0=\Lambda Gb^2LN^2/12C$, and for the drag constant an expression which, in a very crude approximation, leads to $B_1\approx B_c+B_d$. The possibility of an analytic description of the effects can be exploited, as will be done in paper III of the present series of paper, to simplify considerably the discussion of the influence of such external parameters as frequency, temperature, or pinning-point number of internal-friction effects.

Of the various treatments of the drag effect (see paper I), only Simpson and Sosin[7] tried to combine the action of continuous and point-defect drag. However, their treatment resulted in a complicated formalism not well suited to a simple discussion of the effects of the above parameters. For this reason, the present, more transparent treatment of the superposition of the two types of drag effects is not only useful for understanding its physical nature, but is required for its application to the evaluation of experimental data.


## ACKNOWLEDGMENT

This work was begun while one of the authors (A.V.G.) was in Aachen and was completed in Urbana. The work in Urbana is supported by the National Science Foundation under Grant No. NSF DMR80-15707. One of use (A.V.G.) is indebted to the Alexander von Humboldt Striftung for an award which made the visit in Aachen possible.


## APPENDIX A: SUPERPOSITION OF DRAG EFFECTS IN THE RIGID-ROD MODEL

The solution to the system of differential equations, Eqs. (8) and (9), is found by inserting

$$y=\eta\exp(i\omega t),\quad y_d=\eta_d\exp(i\omega t) \tag{A1}$$

in Eqs. (8) and (9) and eliminating $\eta_d$. This leads to the complex displacement amplitude $\eta$:

$$\eta=\frac{\dfrac{b\sigma_0}{K_N}\left[1+i\omega\dfrac{B_d}{K_d}\right]}{\left[1-\omega^2\dfrac{B_cB_d}{K_NK_d}\right]+i\omega\left[\dfrac{B_c}{K_N}+\dfrac{B_d}{K_d}+\dfrac{B_d}{K_N}\right]} . \tag{A2}$$

As shown in Appendix B such an expression can be expressed as a superposition of two relaxation processes with the relaxation times $\tau_{1,2}$ and strengths $\Delta_{1,2}$ given by Eq. (11). Some limit values for these quantities and short indications of the physical meaning of these cases are listed in Table II.

## APPENDIX B: FORM FOR THE SUM OF TWO DEBYE RELAXATIONS

The equation of motion of a dislocation

$$B\dot{y}+Ky-b\sigma_0\exp(i\omega\tau) \tag{B1}$$

($K=$ restoring force constant) leads with $y=\eta\exp(i\omega t)$ to

$$\eta=\frac{b\sigma_0/K}{1+i\omega B/K}=a\frac{1-i\omega\tau}{1+\omega^2\tau^2} . \tag{B2}$$

This describes a simple Debye relaxation (cf. equations of paper I) with

$$\tau=B/K,\quad \Delta=Gb\Lambda a/\sigma_0=Gb^2\Lambda/K .$$

Let us consider the sum of two Debye relaxations:

$$\eta=a_1/(1+i\omega\tau_1)+a_2/(1+i\omega\tau_2) . \tag{B3}$$

This can be written as

$$\eta=(a_1+a_2)\frac{1+i\{[a_1/(a_1+a_2)]\omega\tau_2+[a_2/(a_1+a_2)]\omega\tau_1\}}{(1-\omega^2\tau_1\tau_2)+i\omega(\tau_1+\tau_2)} . \tag{B4}$$

TABLE II. Limit values for relaxation times and strengths for the rigid-rod model. (PD denotes point defect.)

| | $\tau_1/\tau_0$ | $\tau_2/\tau_0$ | $\Delta_1/\Delta_0$ | $\Delta_2/\Delta_0$ | Physical meaning |
|---|---|---|---|---|---|
| $\mu\to 0$ | 1 | $\dfrac{\mu}{\lambda}$ | 1 | $\dfrac{\mu^2}{\lambda}$ | mobile PD |
| $\mu\to\infty$ | $\mu\left[1+\dfrac{1}{\lambda}\right]$ | $\dfrac{1}{1+\lambda}$ | $\dfrac{\lambda}{1+\lambda}$ | $\dfrac{1}{1+\lambda}$ | immobile PD |
| $\lambda\to\infty$ | $1+\mu$ | $\dfrac{\mu/\lambda}{1+\mu}$ | 1 | $\dfrac{\mu^2/\lambda}{(1+\mu)^2}$ | only PD drag (many PD) |
| $\lambda\to 0$ | $\dfrac{\mu}{\lambda}$ | 1 | $\lambda$ | 1 | only continuous drag (no PD) |

This means that an expression of the form

$$\eta = \frac{a(1+ib\omega)}{(1-c\omega^2)+2id\omega} \tag{B5}$$

can always be written in the form of Eq. (B3) with

$$\tau_{1,2} = d \pm (d^2-c)^{1/2} , \tag{B6}$$

$$a_{1,2} = \frac{a}{2}\left[1 \pm \frac{d-b}{(d^2-c)^{1/2}}\right] . \tag{B7}$$

It does not mean, however, that an expression of the form (B5) always represents the superposition of two Debye relaxations. Its physical meaning depends upon the values of the constants. We consider three examples.

(i) To have the sum of two relaxations, one needs $d^2-c>0$ (real relaxation times), $c>0$ and $d>0$ (two positive relaxation times), and $2bd-b^2-c>0$ (two positive relaxation strengths).

(ii) Damped resonance is described by

$$A\ddot{y} + B\dot{y} + Ky = b\sigma_0 \exp(i\omega t) .$$

A is a mass per unit length. With $\omega_0 = K/A$, this leads to

$$\eta = \frac{b\sigma_0}{K}\frac{1}{(1-\omega^2/\omega_0^2)+i\omega B/A\omega_0^2} , \tag{B9}$$

i.e., $a = b\sigma_0/K$, $b=0$, $c=A/K$, $d=B/2K$. For $d^2-c=(B^2/4K^2-A/K)<0$, one has two imaginary relaxation times. This is characteristic of underdamped resonance with a damping maximum at $\omega=\omega_0$.

(iii) For overdamped resonance, i.e., for $(B^2/4K^2-A/K)>0$, one has two real and positive relaxation times, but one negative relaxation strength. This can be seen especially clearly for large overdamping, where

$$\begin{aligned} &\tau_1 = B/K, \quad a_1 = 1 , \\ &\tau_2 = A/B, \quad a_2 = -KA/B^2 . \end{aligned} \tag{B10}$$

The negative second relaxation strength leads to a drop off of damping at high frequencies from the Debye curve corresponding to the first relaxation process, and thus causes the $1/\omega^3$ instead of a $1/\omega$ relationship occurring for overdamped resonance at high frequencies.

## APPENDIX C: SUPERPOSITION OF CONTINUOUS AND DISCRETE DRAG FOR A STRING

Equation (2) can be solved by the trial solution $y(x,t)=\eta(x)\exp(i\omega t)$. If the amplitude $\eta(x)$ is approximated by the zero-order approximation $\eta_0(x)$, its average value is given by

$$\bar{\eta}_0(\omega) = \bar{\eta}_L/(1+i\omega B_c\bar{\eta}_L/b\sigma_0) \tag{C1}$$

as shown by Eq. (B9) of paper I. Here $\eta_L(x)$ is the solution of

$$-C\eta_L'' = b\sigma_0 . \tag{C2}$$

Let us consider first a single pinning point that could be dragged in the middle of a loop $L_N$. Instead of the boundary conditions $\eta(0)=0$, $\eta(L_N)=0$ (Appendix B of paper I), Eq. (C2) must then be solved for the boundary conditions

$$\eta(0)=0, \quad \eta\left[\frac{L_N}{2}\right] = -\frac{2mC}{i\omega}\eta\left[\frac{L_N}{2}\right] . \tag{C3}$$

Equation (C3) follows from the condition $\dot{y}=mF$, where $F$ is the dislocation tension force at the point defect given by $F=-2Cy'$. With the abbreviations

$$A_2 = \frac{b\sigma_0 L_N^2}{2C}, \quad \tau_d = \frac{L_N}{4mC'}, \quad \tau_0 = \frac{B_c L_N^2}{12C} , \tag{C4}$$

Eq. (C2) is solved by

$$\eta_L = A_0 + A_1\frac{x}{L_N} - A_2\frac{x^2}{L_N^2} , \tag{C5}$$

giving for the interval $x = 0 - L_N/2$

$$\bar{\eta}_L = A_0 + A_1/4 - A_2/12 . \tag{C6}$$

The boundary conditions (C3) lead to

$$A_0=0, \quad A_1 = \frac{A_2}{2}\left[\frac{2+i\omega\tau_d}{1+\omega\tau_d}\right] . \tag{C7}$$

Inserting Eqs. (C4), (C6), and (C7) into (C1) finally gives

$$\bar{\eta}_0 = \frac{(b\sigma_0 L_N^2/12C)(1+i\omega\tau_d/4)}{(1-\omega^2\tau_d\tau_0/4)+i\omega(\tau_0+\tau_d)} . \tag{C8}$$

According to Appendix B this corresponds to a sum of two relaxations. With

$$\Delta_{1,2} = \frac{\Lambda G b}{\sigma_0}a_{1,2}, \quad \Delta_0 = \frac{\Lambda G b^2 L_N^2}{12}C' , \tag{C9}$$

the relaxation times and strengths are given by Eqs. (B6) and (B7) as

$$\tau_{1,2}=\tfrac{1}{2}\{(\tau_0+\tau_d)\pm[(\tau_0+\tau_d)^2-\tau_0\tau_d]^{1/2}\}\ , \tag{C10a}$$

$$\Delta_{1,2}=\frac{\Delta_0}{2}\left[1\pm\frac{\tau_0+\tau_d/2}{[(\tau_0+\tau_d)^2-\tau_0\tau_d]^{1/2}}\right] . \tag{C10b}$$

From this derivation, it may be inferred that for $n-1$ pinners

$$\tau_{1,2}=\frac{1}{2}\left[(\tau_0+\tau_d)\pm\left[(\tau_0+\tau_d)^2-\frac{4}{n^2}\tau_0\tau_d\right]^{1/2}\right], \tag{C11a}$$

$$\Delta_{1,2}=\frac{\Delta_0}{2}\left[1\pm\frac{\tau_0+\left[1-\dfrac{2}{n^2}\right]\tau_d}{\left[(\tau_0+\tau_d)^2-\dfrac{4}{n^2}\tau_0\tau_d\right]^{1/2}}\right], \tag{C11b}$$

where now $\tau_d$ has been redefined to be [cf. Eq. (9) of paper I]

$$\tau_d=\frac{B_d L_N^2}{12C\gamma_0(n)}=\frac{(n+1)L_N}{12mC'} \tag{C12}$$

with $B_d$ given by Eq. (6) and $\gamma_0(n)=n/(n+1)$ as given by Table I of paper I. With Eq. (C4) for $\tau_0$ and Eq. (C12), Eqs. (C11) lead directly to the Eqs. (19) and (20) in the text.

[1]K. Lücke and A. Granato, referred to as paper I, preceding paper, Phys. Rev. B 24, 6991 (1981).
[2]A. Granato and K. Lücke, J. Appl. Phys. 27, 583, (1956); 27, 789 (1956).
[3]A. Granato and K. Lücke, in *Physical Acoustics*, edited by W. P. Mason (Academic, New York, 1960), Vol. IVa, p. 266.
[4]E. Lenz and K. Lücke, in *Internal Friction and Ultrasonic Attentuation in Solids*, edited by D. Lenz and K. Lücke (Springer, Berlin, 1975), Vol. II, p. 48.
[5]K. Lücke, A. Schnell, and G. Sokolowski (unpublished).
[6]A. Granato, in *Fundamental Aspects of Radiation Damage in Metals*, edited by M. T. Robinson and F. W. Young, Jr. (National Technical Information Service, U. S. Dept. of Commerce, Springfield. Va., 1975), CONF-751006-P1, Vol. II, p. 932.
[7]H. M. Simpson and A. Sosin, Phys. Rev. B 5, 1382 (1972); 16, 1489 (1977).